Catalyst- and Silane-Controlled Enantioselective Hydrofunctionalization of Alkenes by Cobalt-Catalyzed Hydrogen Atom Transfer and Radical-Polar Crossover

Kousuke Ebisawa, Kana Izumi, Yuka Ooka, Sayori Kanazawa, Sayura Komatsu, Eriko Nishi, Hiroki Shigehisa*

Faculty of Pharmacy, Musashino University, 1-1-20 Shinmachi Nishitokyo-shi, Tokyo 202-8585, Japan

ABSTRACT: Catalytic enantioselective synthesis of tetrahydrofurans, which are found in the structures of many biologically active natural products, via a transition-metal catalyzed-hydrogen atom transfer (TM-HAT) and radical-polar crossover (RPC) mechanism is described herein. Hydroalkoxylation of non-conjugated alkenes proceeded efficiently with excellent enantioselectivity (up to 94% ee) using a suitable chiral cobalt catalyst, *N*-fluoro-2,4,6-collidinium tetrafluoroborate, and diethylsilane. Surprisingly, absolute configuration of the product was highly dependent on the steric hindrance of the silane. Slow addition of the silane, the dioxygen effect in the solvent, thermal dependency, and DFT calculation results supported the unprecedented scenario of two competing selective mechanisms. For the less-hindered diethylsilane, a high concentration of diffused carbon-centered radicals invoked diastereoenrichment of an alkylcobalt(III) intermediate by a radical chain reaction, which eventually determined the absolute configuration of the product. On the other hand, a more hindered silane resulted in less opportunity for radical chain reaction, instead facilitating enantioselective kinetic resolution during the late-stage nucleophilic displacement of the alkylcobalt(IV) intermediate.

Introduction

The transition-metal-catalyzed-hydrogen atom transfer (TM-HAT) of alkenes has recently attracted significant attention in synthetic organic chemistry.[1] Originally, Halpern proposed the transfer of a hydrogen atom from a cobalt hydride species for the hydrogenation of anthracene.[2] A few years later, Halpern (Mn)[3] and Marko (Co)[4] reported the hydrogenation of styrenes and established the TM-HAT mechanism using kinetic and spectroscopic experiments. Independently, Drago[5] and Mukaiyama[6] reported the catalytic hydration of alkenes under aerobic conditions. These alkene-chemoselective reactions and their modifications have been recently used in the synthesis of complex molecules, such as natural products.[1b,7] The catalytic hydrations have now been advanced to applications in diverse hydrofunctionalization and other useful transformations (**Figure 1a, left**)[8,9]. The mechanism of these relevant reactions is also becoming clearer.[9n,9r,10]

Our group has previously reported diverse hydrofunctionalizations using a cobalt Schiff base catalyst, *N*-fluorocollidinium salt, and a silane reagent (**Figure 1a, right**).[11] A remarkable and unique mechanistic feature of this reaction is that the radical species generated by TM-HAT was transformed via single-electron oxidation into a cationic species that can receive various nucleophiles. This radical-polar crossover (RPC) mechanism enabled the protonation of alkenes without a proton source, realizing excellent chemoselectivity and functional group tolerance.

Despite numerous reports and our previous preliminary results,[11c] high enantioselectivity for the hydrofunctionalization of alkenes based on a TM-HAT reaction mechanism had not been reported until recently (**Figure 1b**).[12] Such difficulty is unsurprising given the inherently challenging construction of a chiral carbon from a reactive prochiral radical center. However, Pronin and coworkers eventually reported the highly enantioselective formation of epoxides from a tertiary allylic alcohol by a TM-HAT and RPC approach using a finely tuned cobalt comp lex.[13] Importantly, they proposed the presence of an

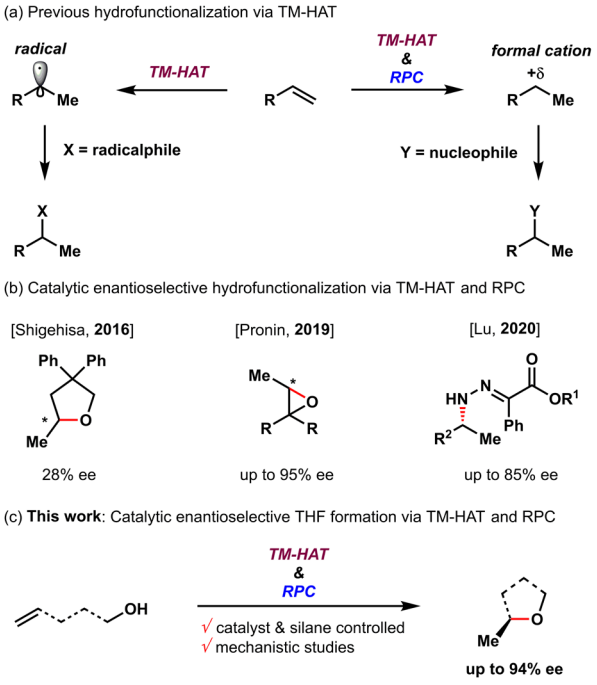

Figure 1. Previous examples and this work

Table 1. Screening of cobalt catalysts and silanes[a]

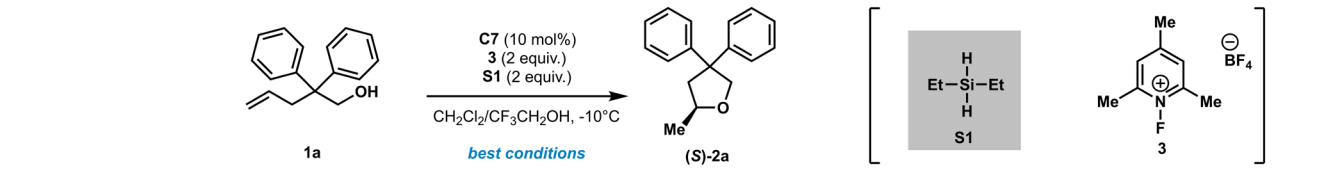

(a) catalyst[b]

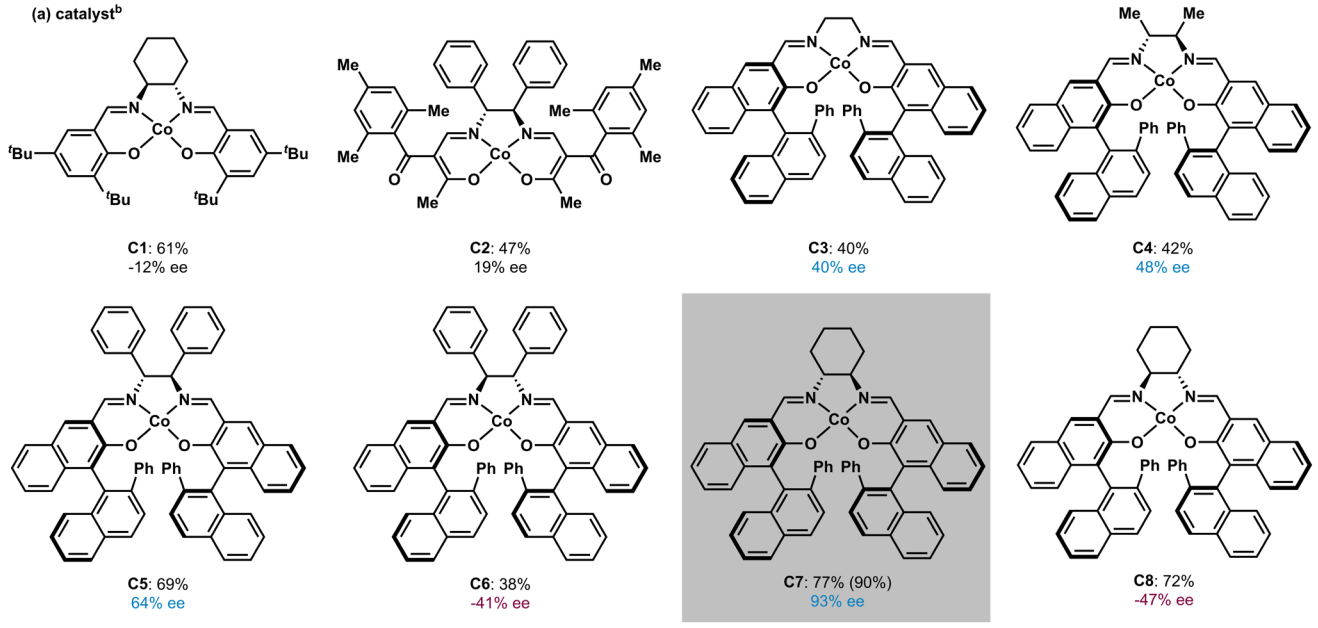

C1: 61%, -12% ee
C2: 47%, 19% ee
C3: 40%, 40% ee
C4: 42%, 48% ee
C5: 69%, 64% ee
C6: 38%, -41% ee
C7: 77% (90%), 93% ee
C8: 72%, -47% ee

(b) silanes[b]

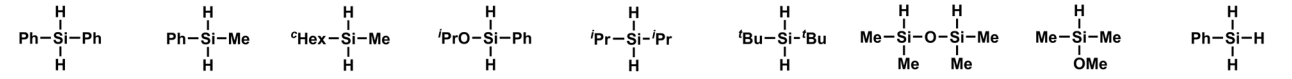

S2: 74%, 85% ee
S3: 71%, 82% ee
S4: 68% (81%), 78% ee
S5: 60%, 65% ee
S6: 18% (23%), -50% ee
S7: No reaction
S8: 53% (53%), -58% ee
S9: 69% (77%)[c], -22% ee
S10: 59% (64%), 1% ee

Best conditions: **1a** (0.1 mmol), **C7** (10 mol%), **3** (2 equiv.), diethylsilane (**S1**, 2 equiv.), CH_2Cl_2 (4.0 mL), CF_3CH_2OH (0.2 mL), −10 °C, 30 min (the same result was obtained after 24 h), 77% [a]Reaction times for experiments under conditions other than the optimum ones were 24–36 h (see SI). [b]Isolated yields are shown. The yield in parentheses is an NMR yield using 1,4-bis-trifluoromethylbenzene as the internal standard. [c]4 equiv. of silane.

alkylcobalt(IV) intermediate with the contribution of a cation–π interaction in the asymmetric induction. More recently, Lu reported enantioselective hydrazone formation initiated by TM-HAT.[14]

Since we obtained our preliminary result of enantioselectivity,[11c] we have been extensively exploring alternative reaction conditions to improve the reaction. Eventually, we found the high enantioselectivity of our catalytic hydroalkoxylation of unactivated alkenes afforded chiral tetrahydrofurans, which are found in the structures of many biologically active natural products, via a TM-HAT and RPC approach (**Figure 1c**).[15] Herein, we describe the process leading to the optimal reaction conditions of a chiral cobalt catalyst, *N*-fluoro-2,4,6-collidinium tetrafluoroborate, and diethylsilane. To our surprise, the absolute configuration of the product was highly dependent on the steric hindrance of the silane reagent, which is typically viewed as a hydrogen source for the cobalt hydride species. This silane-controlled product selectivity is unique in TM-HAT chemistry. Therefore, we experimentally and computationally examined the mechanism of this catalysis and the unique silane effect.

Results and Discussion

We started to explore the enantioselective hydroalkoxylation of alkenyl alcohol **1a** (>200 runs, >30 cobalt catalysts, and >20 silanes) and identified the optimal reaction conditions as the use of the cobalt catalyst **C3** (10 mol%),[16] *N*-fluoro-2,4,6-collidinium tetrafluoroborate,[17] and diethylsilane in dichloromethane/trifluoroethanol (20:1)[18] at -10 °C to afford cyclic ether (*S*)-**2a** in excellent yield and enantioselectivity (**Table 1**).[19] Screening of various chiral cobalt complexes revealed that the bulky ligands (**C3**–**C8**) reported by Katsuki are preferable to the simpler salen ligand (**C1**)[20] or β-ketoiminate ligand (**C2**).[21] Notably, the axial chirality of the binaphthyl unit had a significant impact on the enantioselectivity; even **C3**, lacking chirality on the diamine, provided higher enantioselectivity than **C1** or **C2**. The introduction of two methyl groups on the diamine (**C4**) did not sufficiently improve the enantioselectivity; however, enantioselectivities were enhanced for diphenyl (**C5**) or cyclohexyl (**C7**) diamines, probably by further locking the conformation of the ligand. The conformation of the ligand is crucial for reactivity and enantioselectivity, as also reflected by the significantly worse results obtained upon using the diastereomers

Table 2. Substrate scope of enantioselective hydroalkoxylation of alkenyl alcohol

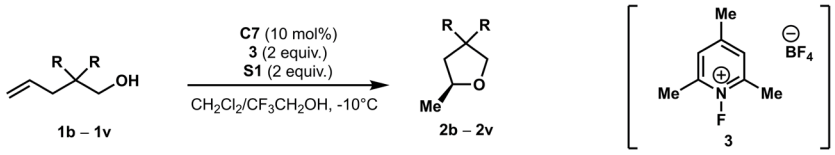

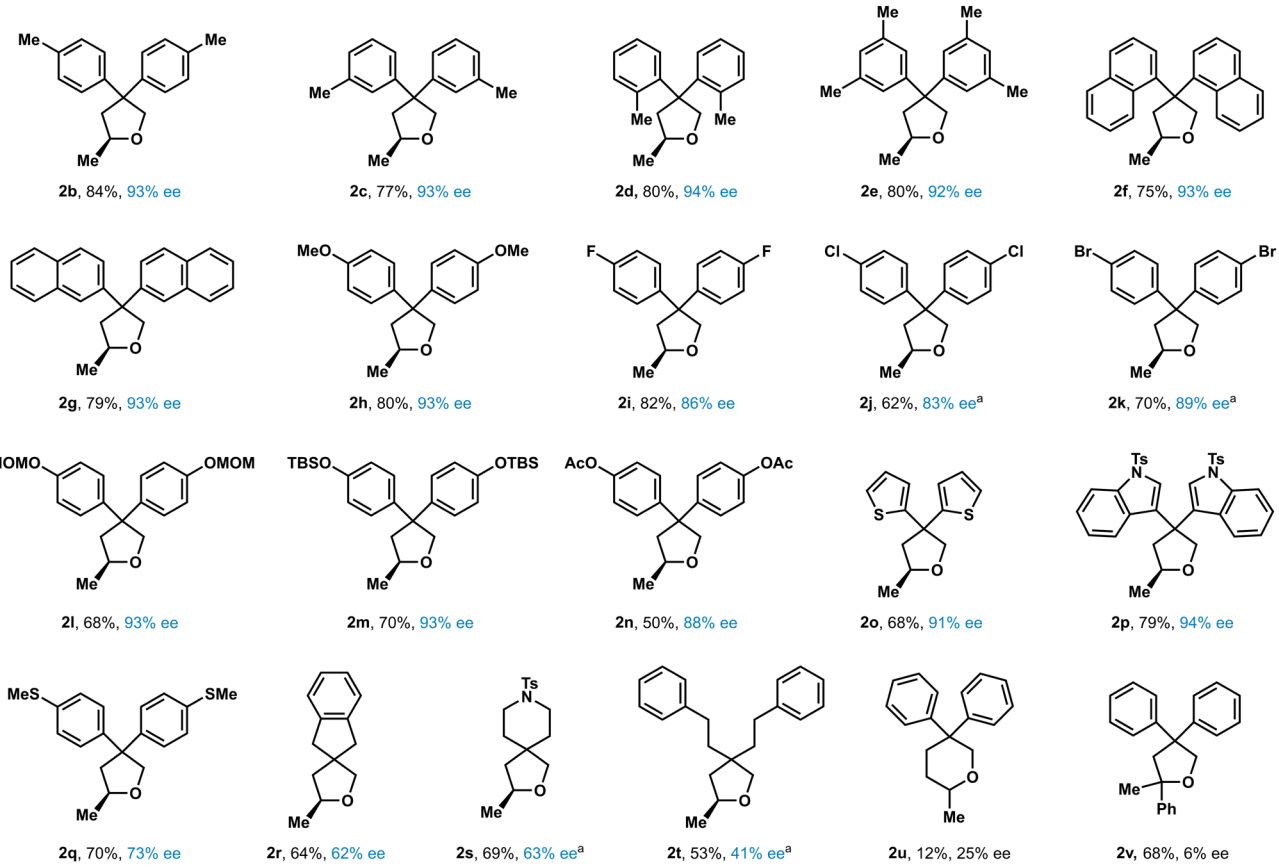

Conditions: **1b-t** (0.1 mmol), **C3** (10 mol %), **3** (2 equiv.), diethylsilane (2 equiv.), CH_2Cl_2 (4.0 mL), CF_3CH_2OH (0.2 mL), −10 °C, 16 h. Isolated yields are shown. [a]temperature = −20 °C.

C6 and **C8**. Extensive screening showed that silane reagents had significant impact on the enantioselectivity.[22] A secondary silane was essential for obtaining the excellent enantioselectivity of (*S*)-**2a**. Among secondary silanes, the sterically least hindered diethylsilane (**S1**) was found to be optimal. To our surprise, the use of the sterically more hindered diisopropylsilane (**S6**) afforded (*R*)-**2a** as the major enantiomer. This result is remarkable because in the typical TM-HAT mechanism, the silane reagent acts as a hydrogen source for the cobalt hydride species, and is not directly involved in the asymmetric induction. The more hindered di-*tert*-butylsilane (**S7**) resulted in no reaction of **1a**. The stereochemistry of the major enantiomer formed using a tertiary silane (**S8** and **S9**) was also (*R*)-**2a**, which is the same as that when using **S6**. A primary silane afforded a near racemate.[23] Therefore, steric hindrance of the silane determined the absolute configuration of the product.

After establishing the optimal reaction conditions, we explored the scope of the enantioselective hydroalkoxylation with various alkenyl alcohols (**Table 2**). We commenced with the examination of the steric effects by introducing a methyl group on the phenyl rings, and found no significant difference in the results obtained with 4-methyl (**2b**), 3-methyl (**2c**), 2-methyl (**2d**), 3,5-xylyl (**2e**), 1-naphthyl (**2f**), and 2-naphthyl (**2g**) substitutions. We next investigated the electronic effect of the aromatic ring. While the introduction of a methoxy group did not change the yield or enantioselectivity (**2h**), introduction of a halogen substituent slightly decreased the enantioselectivity (**2i**-**2k**). Examination of the functional group tolerance of this reaction revealed that the product could be obtained from alkenyl alcohols bearing an acid-sensitive acetal (**2l**), fluoro-anion-sensitive silyl ether (**2m**), or base-sensitive acetate (**2n**). Replacing the phenyl ring with heterocycles such as thiophene (**2o**) or *N*-tosyl indole (**2p**) resulted in comparable yields and enantioselectivities. Unfortunately, introducing a methylthio group (**2q**) or other subunits such as indane (**2r**), *N*-Ts-piperidine (**2s**), or bisphenethyl (**2t**) in place of the diaryl groups reduced the enantioselectivity. Reactions forming a 6-membered ring (**2u**, low conversion), using a disubstituted alkene (**2v**, low conversion), or using a MOM-protected alkenyl alcohol (**2b**, 16%, 1% ee) were found to be ineffective under our conditions.

The proposed reaction pathways depicted in **Figure 2** are consistent with those found in the literature. As postulated for the cobalt(III) hydride-HAT to alkenes,[24] a caged radical-catalyst pair **4** initially forms.[9n,9r,25] Subsequently, bifurcation of the reaction would be possible as follows: (1) the formation of cage-collapsed alkylcobalt(III) complex **5**, followed by single-electron oxida-

tion[26] to generate scalemic alkylcobalt(IV) intermediate **6**;[10a,11f,13,27] or (2) the pair collapse is bypassed and the escaped diffused radical **4′** is captured by a cationic cobalt(III) complex, whereupon the pathways converge to the key alkylcobalt(IV) intermediate **6**.[28] The C–O bond would be formed by nucleophilic displacement with stereoinversion to afford **7** instead of the tentative formation of a planar carbocation.[11d,13,27c,27d,27g] Finally, deprotonation of **7** by 2,4,6-collidine would afford product **2**.

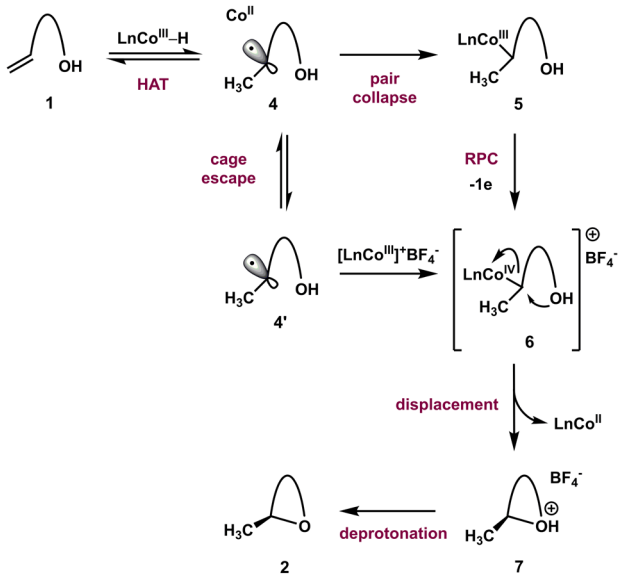

Figure 2. Proposed mechanism

With a reasonable reaction mechanism in hand, the possible enantiodetermining steps are discussed individually (**Figure 3**) as follows.

(A) A first possibility is the enantiodetermining formation of an alkylcobalt(III) complex from a cobalt(II) complex and carbon-centered radical, creating a stereocenter on the corresponding carbon atom. This process can occur within the solvent cage or after cage escape.

(B) Formation of an alkylcobalt(IV) complex from a cationic cobalt(III) complex and a diffused carbon-centered radical also generates a stereocenter on the corresponding carbon atom. Pronin suggested this enantiodetermining step as one possibility in their reaction.[13]

(C) Even once the alkylcobalt(III) complex is formed, a diffused carbon-centered radical can react with the alkylcobalt(III) complex by homolytic displacement (S_H2); this radical chain reaction gives rise to an equilibrium between two diastereomeric alkylcobalt(III) complexes, and converges on the specific stable complex. Originally, Kochi reported the alkyl rearrangement of an alkylcobalt complex by a radical chain reaction.[29] Wayland also experimentally and computationally examined a cobalt-catalyzed living radical polymerization, including a radical chain mechanism.[30]

(D) A last possibility is an enantiodetermining nucleophilic displacement of the alkylcobalt(IV) complex to afford a cyclic ether product. There can be some degree of energetic difference between the two transition states derived from each diastereomeric alkylcobalt(IV) complex. Pronin further suggested such an enantioselective kinetic resolution in addition to hypothesis (B).[13]

Given the enantiodiversity of the resultant cyclic ether, it is assumed that our enantioselective catalysis might contain no fewer than two enantiodetermining steps among these four scenarios. In the following sections, we discuss the refinement of these hypotheses (**Figure 3**) experimentally and computationally, elucidating the silane effect.

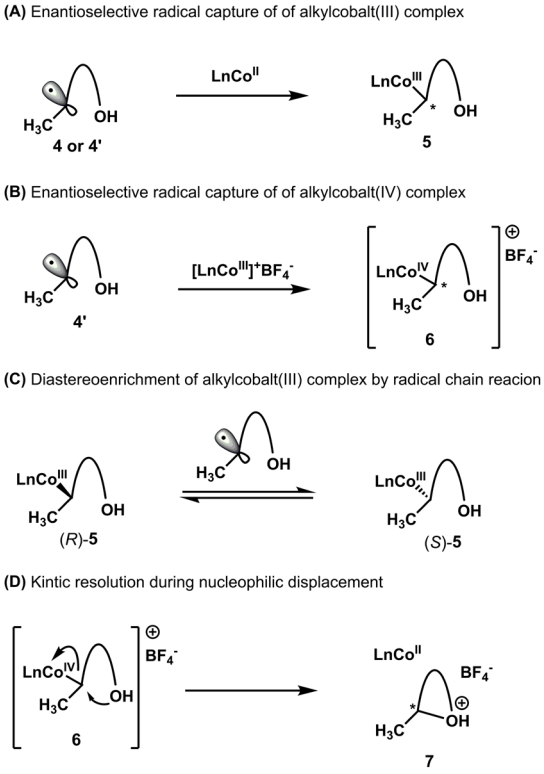

Figure 3. Hypothetical enantiodetermining steps

Silane screening (**Table 1**) indicated that the steric hindrance of the silane reagent was dramatically crucial for the absolute configuration of the product and its degree of enantioselectivity. To examine the role of the silane reagent in more detail, we controlled the concentration of silane reagent in the solution by its slow addition (**Table 3**). The enantioselectivities using secondary silanes such as **S1** and **S4**, providing (*S*)-**2a** as the major enantiomer, were reduced from 93% and 78% ee to 80% and 61% ee, respectively, when slow addition was used (entries 2, 4). Furthermore, the addition of **S4** over 80 h changed the major enantiomer from (*S*)-**2a** to (*R*)-**2a** (entry 5). On the other hand, the enantioselectivity using hindered silane **S8**, providing (*R*)-**2a** as the major enantiomer, increased from 58% to 69% ee by slow addition over 2 h (entry 7).

These results clearly indicate that no fewer than two enantiodetermining steps were competing in the cobalt catalysis. The relative contribution of the steps seems to depend on the concentration of silane reagent and the downstream intermediates. Apparently, the smallest silane, **S1**, which has the shortest reaction time among all the silane reagents, has the highest reactivity and generates the highest concentration of the downstream intermediates. For example, a hypothetical radical chain reaction (C) fits the experimental results; the rate of the radical

chain reaction disproportionation to the more stable scalemic alkylcobalt(III) intermediate should depend on the concentration of a diffused carbon-centered radical and alkylcobalt(III) intermediate. Conversely, the reaction with hindered silane **S8** would include minimal influence of a radical chain. The slightly higher enantioselectivity from the slow addition would result from attenuation of the radical chain contribution; the concentration of intermediates might not affect the enantiodetermining step leading to (*R*)-**2a**. This would be understandable in view of intramolecular displacement (D), independent of the concentration of carbon centered radical. However, the contributions of hypotheses (A) and (B) to the enantioselectivity should not be completely ruled out.

Table 3. Mechanistic experiments

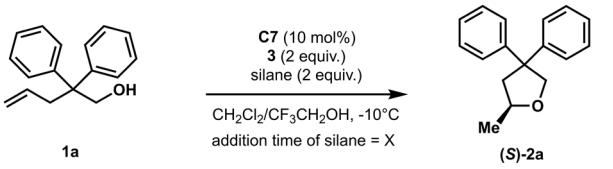

1a **(*S*)-2a**

entry	silane	remark	time[b]	yield (%)[a]	ee (%)
1	**S1**	X = one shot	20 m	90	93
2	**S1**	X = 2 hours	2 h	87	80
3	**S4**	X = one shot	4 h	81	78
4	**S4**	X = 2 hours	4 h	79	61
5	**S4**	X = 80 hours	80 h	36	-14
6	**S8**	X = one shot	36 h	53	-58
7	**S8**	X = 2 hours	36 h	60	-67
8	**S1**	Non-deoxygenated CF_3CH_2OH	18 h	71	72
9	**S8**	Non-deoxygenated CF_3CH_2OH	36 h	55	-59

[a]Yields based on GC using 1,3,5-tri-tert-butylbenzene as an internal standard. [b]Each reaction time was measured from the start of the addition.

During the optimization of reaction conditions using **S1**, we found that deoxygenation of the solvent is crucial for high enantioselectivity. Indeed, the run without deoxygenation of trifluoroethanol decreased the enantioselectivity from 93% to 72% ee (**Table 3**, entry 8). This result is understandable because dioxygen can quench the carbon-centered radical. The inhibition of a radical chain reaction in a cobalt-catalyzed reaction was previously reported by Kochi.[29]

On the other hand, the enantioselectivity using **S8** was not affected by dioxygen (entry 9). This result supports step (D), where there is no involvement of carbon-centered radical, as the enantiodetermining step leading to (*R*)-**2a**.

We next investigated the thermal dependency of the enantioselectivity by comparing **S1** and **S8** (**Figure 4**). It is traditionally considered that a lower temperature improves enantioselectivity.[31] However, we found that the situation for **S1** is not simple; the ee variation was not monotonic with the temperature. The slightly convex Eyring plot is characterized by two lines with an inversion point (T_{inv} = −10 °C). On the other hand, using **S8** resulted in a typical rising linear Eyring plot.

The nonlinearity for **S1** is generally interpreted as evidence for a reaction pathway with at least two enantiodetermining steps weighted differentially according to the temperature.[32] If radical chain reaction (C) occurs, we should consider the possibilities of 1) an energetically positive effect toward the diastereomeric ratio of the alkylcobalt(III) intermediate at lower temperature, 2) a negative effect toward the radical chain by interruption of the cage escape in the higher viscosity of the solvent at lower temperature,[33] and 3) a higher selectivity of competing enantiodetermining steps leading to (*R*)-**2a** at lower temperature. A balance of these factors would result in the unusual Eyring plot. For **S8**, the derived activation parameters indicated that the differential enthalpy is a major contributor to the enantiodetermining step. It is to be noted that the Eyring plot for **S8** and the derived activation parameters might entail the influence of a radical chain reaction, as indicated from the silane-slow addition experiment. If so, in view of the slightly dropping regression line of the Eyring plot of **S1**, the actual differential enthalpy of the related enantiodetermining step could be slightly higher. Pronin ruled out enantioselective radical capture (A) because of its considerably larger differential enthalpy compared with the known activation enthalpy of a diffusion-controlled process (2 kcal/mol).[13] Even though our differential enthalpy is close to the value of 2 kcal/mol, it remains uncertain whether hypothesis (A) can be ruled out because of the partial influence of the radical chain reaction.

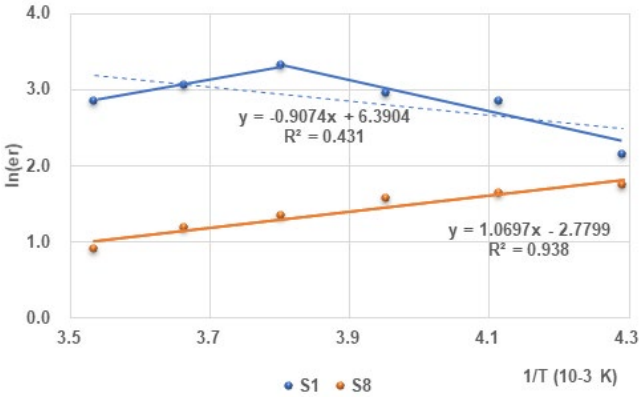

Figure 4. Eyring plots. Activation parameters calculated from these Eyring plots were $\Delta\Delta H^{\ddagger}$ = −2.13 kcal/mol and $\Delta\Delta S^{\ddagger}$ = −5.53 kcal/mol·K for **S1,** and $\Delta\Delta H^{\ddagger}$ = 1.81 kcal/mol and $\Delta\Delta S^{\ddagger}$ = 12.7 kcal/mol·K for **S8**.

To gain additional insight into the mechanism and enantioselectivity, we next performed density functional theory (DFT) studies, commencing with the Co–C bond formation affording alkylcobalt(III) complex **5**. The transition state was searched by elongating the Co–C bond of the alkylcobalt complex. For complex **5**, only a regular increase in energy was observed until the complete dissociation. Wayland reported, in the same process for their cobalt catalysis, that there is no transition state (barrierless) on the electronic energy surface and this process requires mostly an entropic contribution to bring together the radical and cobalt complex.[34] Given the Eyring study using **S8**, our calculated result is inconsistent with a rising linear plot, which indicates an enthalpically controlled process.

On the other hand, we found the transition state of the Co–C bond formation affording alkylcobalt(IV) complex **6** by the same approach as that used for **5**. Transition state (*R*)-**TS1a**, leading to (*S*)-**2a**, is 0.91 kcal/mol more stable than (*S*)-**TS1a** (See Supporting Information for detail). This result might indicate enantiodetermining bond formation of alkylcobalt(IV) complex **6** leading to (*S*)-**2a**; however, the energetic difference is too small to explain quantitatively.

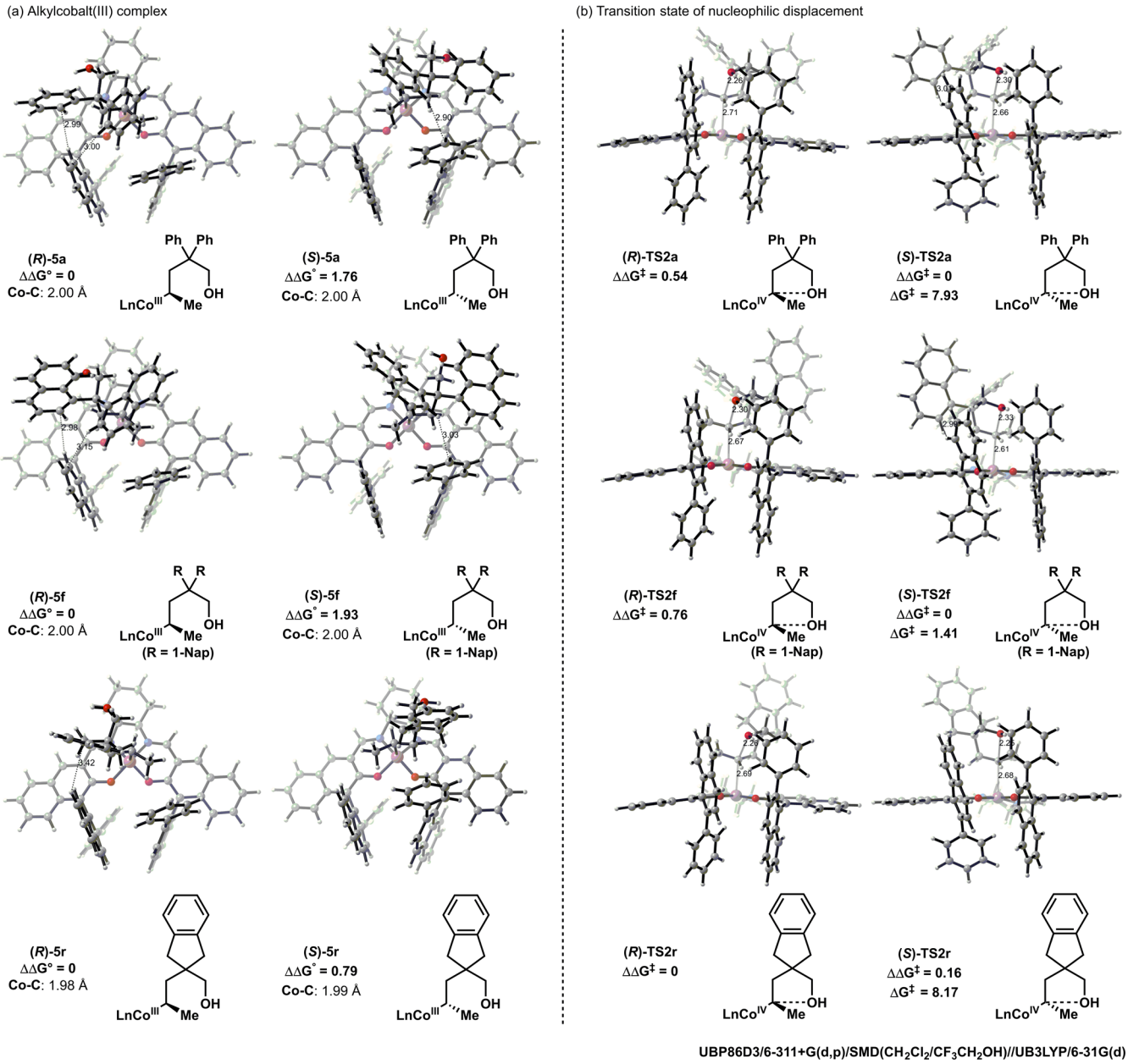

Figure 5. (A) Lowest-energy diastereomeric alkylcobalt(III) complex (B) Lowest-energy TSs of nucleophilic displacement. All energies are in kcal mol^{-1}.

To further validate the radical chain reaction leading to (*S*)-**2a** using **S1**, we computed the energetic difference of diastereomeric alkylcobalt(III) intermediate **5** (**Figure 5**). The energy of (*R*)-**5a**, leading to (*S*)-**2a**, was 1.76 kcal/mol lower than that of (*S*)-**5a**. This difference in energy agrees with the enantioselectivity observed for (*S*)-**2a**. Apparently, there are favorable noncovalent interactions between the aromatic rings (naphthyl and phenyl) of the ligand and the two phenyl groups of the substrate.[35] Indeed, the difference in energy is smaller for the diastereomers **5r** (0.79 kcal/mol) than for the diastereomers **5f** (1.93 kcal/mol). They are also in nearly quantitative agreement with the experimentally observed enantioselectivities of **2r** (62% ee) and **2f** (93% ee).

We next computed the energies of the diastereomeric transition states of the nucleophilic displacement at the same level of theory. The detailed geometry optimization revealed that the Co–C bond needed to be rotated from the geometry of the alkylcobalt(III) complex to obtain the transition state. The transition state (*R*)-**TS2a**, leading to (*S*)-**2a**, is 0.54 kcal/mol less stable than (*S*)-**TS2a**. This result clearly reflects the preference of affording (*R*)-**2a** using **S8**. In addition, the relative Gibbs free energy between the diastereomeric transition states correlated with the bond length of the Co–C bond. The difference in energy is larger for **TS2f** (0.76 kcal/mol) and smaller for the diastereomeric transition state **TS2r** (0.16 kcal/mol). The difference between these values, less than 1 kcal/mol, is not high enough for quantitative discussion. However, this result is qualitatively consistent with the enantioselectivities of **2f** and **2r** using **S8** (72% ee and 32% ee, respectively). In the structures of (*S*)-**TS2a** and (*S*)-**TS2f**, we found the same noncovalent interaction between the aromatic rings of the ligand and substrate as was observed in (*R*)-**5a**. Together, the corresponding noncova-

lent interactions would be the origin of the enantiodetermining for not only the diastereomeric alkylcobalt(III) complex, but also the transition state of the nucleophilic displacement.

Conclusion

We developed a catalytic enantioselective synthesis of tetrahydrofurans via a cobalt-catalyzed HAT/RPC approach. Intramolecular hydroalkoxylation of an alkenyl alcohol proceeded efficiently with excellent enantioselectivity using chiral cobalt catalyst **C7**, *N*-fluoro-2,4,6-collidinium tetrafluoroborate, and diethylsilane. A series of chiral tetrahydrofurans were synthesized by this method. The absolute configuration of the product was found to depend on the bulkiness of the silane used.

According to silane-slow addition and deoxygenation experiments, the concentration of intermediates such as a carbon-centered radical influences the absolute configuration of the product. The DFT calculations provided a plausible explanation for the catalyst- and silane-controlled enantioselectivity. After HAT, the unselective pair collapse would form a racemic alkylcobalt(III) intermediate. Use of a small secondary silane, represented by **S1**, invoked an extensive radical chain reaction between the alkylcobalt(III) intermediate and a diffused carbon-centered radical disproportionating to the scalemic (*R*)-**5a**. The biased intermediate finally led to the major product (*S*)-**2a** in excellent enantioselectivity. On the other hand, using a bulky silane such as **S8** resulted in the radical chain reaction being less dominant, the racemic alkylcobalt(III) intermediate remaining nearly unchanged, and kinetic resolution by the moderately enantioselective nucleophilic displacement leading to the opposite enantiomer (*R*)-**2a**. These statements are consistent with the Eyring plots.

This scenario of competing mechanisms is unprecedented for enantioselective TM-HAT chemistry, and further development is warranted to take full advantage of this selectivity. Expansion of the substrate scope of the enantioselective hydrofunctionalization by the RPC mechanism and detailed mechanistic studies are currently ongoing.

Associated Content

Supporting Information. Experimental procedures and analytical data (^{1}H and ^{13}C NMR) for all new compounds. This material is available free of charge via the Internet at http://pubs.acs.org.

AUTHOR INFORMATION

Corresponding Author

*cgehisa@musashino-u.ac.jp.

Funding Sources

This work was supported by JSPS KAKENHI Grant number 17K15426, the Uehara memorial foundation, Takeda Science Foundation, Takeda Award in Synthetic Organic Chemistry, japan, the research foundation for pharmaceutical sciences.

Notes

The authors declare no competing financial interest.

ACKNOWLEDGMENT

We thank Kou Hiroya (Musashino university) for our liberal research environment. We thank Masahiro Anada (Musashino university) for chiral columns. We thank Dr Sumie Tajima (HULINKS Ink) and Hiroyuki Morimoto (Kyushu University) for the helpful advice of DFT calculations. The computation was carried out using the computer facilities at Research Institute for Information Technology, Kyushu University. Dedicated to the memory of Professor Tsutomu Katsuki, Jack Halpern, Teruaki Mukaiyama, and Tadaharu Shigehisa.

REFERENCES

1. (a) Green, S. A.; Crossley, S. W. M.; Matos, J. L. M.; Vásquez-Céspedes, S.; Shevick, S. L.; Shenvi, R. A., The High Chemofidelity of Metal-Catalyzed Hydrogen Atom Transfer. *Acc. Chem. Res.* **2018**, *51,* 2628-2640; (b) Crossley, S. W.; Obradors, C.; Martinez, R. M.; Shenvi, R. A., Mn-, Fe-, and Co-Catalyzed Radical Hydrofunctionalizations of Olefins. *Chem. Rev.* **2016**, *116,* 8912-9000; (c) Shenvi, R. A. M., J. L. M.; Green, S. A, Hydrofunctionalization of Alkenes by Hydrogen-Atom Transfer. *Organic Reactions* **2020**, 383-470.

2. Feder, H. M.; Halpern, J., Mechanism of the cobalt carbonyl-catalyzed homogeneous hydrogenation of aromatic hydrocarbons. *J. Am. Chem. Soc.* **1975**, *97,* 7186-7188.

3. Sweany, R. L.; Halpern, J., Hydrogenation of α-methylstyrene by hydridopentacarbonylmanganese (I). Evidence for a free-radical mechanism. *J. Am. Chem. Soc.* **1977**, *99,* 8335-8337.

4. Ungvary, F.; Marko, L., Reaction of $HCo(CO)_4$ and CO with styrene. Mechanism of (α-phenylpropionyl)- and (β-phenylpropionyl)cobalt tetracarbonyl formation. *Organometallics* **1982**, *1,* 1120-1125.

5. Zombeck, A.; Hamilton, D. E.; Drago, R. S., Novel catalytic oxidations of terminal olefins by cobalt(II)-Schiff base complexes. *J. Am. Chem. Soc.* **1982**, *104,* 6782-6784.

6. Teruaki, M.; Shigeru, I.; Satoshi, I.; Koji, K.; Tohru, Y.; Toshihiro, T., Oxidation-Reduction Hydration of Olefins with Molecular Oxygen and 2-Propanol Catalyzed by Bis(acetylacetonato)cobalt(II). *Chem. Lett.* **1989**, *18,* 449-452.

7. (a) Godfrey, N. A.; Schatz, D. J.; Pronin, S. V., Twelve-Step Asymmetric Synthesis of (−)-Nodulisporic Acid C. *J. Am. Chem. Soc.* **2018**, *140,* 12770-12774; (b) Thomas, W. P.; Schatz, D. J.; George, D. T.; Pronin, S. V., A Radical-Polar Crossover Annulation To Access Terpenoid Motifs. *J. Am. Chem. Soc.* **2019**, *141,* 12246-12250; (c) Hu, X.; Maimone, T. J., Four-step synthesis of the antimalarial cardamom peroxide via an oxygen stitching strategy. *J. Am. Chem. Soc.* **2014**, *136,* 5287-5290.

8. Isayama, S.; Mukaiyama, T., A New Method for Preparation of Alcohols from Olefins with Molecular Oxygen and Phenylsilane by the Use of Bis(acetylacetonato)cobalt(II). *Chem. Lett.* **1989**, *18,* 1071-1074.

9. (a) Waser, J.; Carreira, E. M., Convenient synthesis of alkylhydrazides by the cobalt-catalyzed hydrohydrazination reaction of olefins and azodicarboxylates. *J. Am. Chem. Soc.* **2004**, *126,* 5676-5677; (b) Waser, J.; Nambu, H.; Carreira, E. M., Cobalt-Catalyzed Hydroazidation of Olefins: Convenient Access to Alkyl Azides. *J. Am. Chem. Soc.* **2005**, *127,* 8294-8295; (c) Waser, J.; Gaspar, B.; Nambu, H.; Carreira, E. M., Hydrazines and Azides via the Metal-catalyzed Hydrohydrazination and Hydroazidation of Olefins. *J. Am. Chem. Soc.* **2006**, *128,* 11693-11712; (d) Gaspar, B.; Carreira, E. M., Cobalt Catalyzed Functionalization of Unactivated Alkenes: Regioselective Reductive C-C Bond Forming Reactions. *J. Am. Chem. Soc.* **2009**, *131,* 13214-13215; (e) Ishikawa, H.; Colby, D. A.; Seto, S.; Va, P.; Tam, A.; Kakei, H.; Rayl, T. J.; Hwang, I.; Boger, D. L., Total Synthesis of Vinblastine, Vincristine, Related Natural Products, and Key Structural Analogues. *J. Am. Chem. Soc.* **2009**, *131,* 4904-4916; (f) Barker, T. J.; Boger, D. L., Fe(III)/$NaBH_4$-mediated free radical hydrofluorination of unactivated alkenes. *J. Am. Chem. Soc.* **2012**, *134,* 13588-13591; (g) Leggans, E. K.; Barker, T. J.; Duncan, K. K.; Boger, D. L., Iron(III)/$NaBH_4$-mediated Additions to Unactivated Alkenes: Synthesis of Novel

20'-vinblastine Analogues. *Org. Lett.* **2012**, *14,* 1428-1431; (h) Lo, J. C.; Gui, J.; Yabe, Y.; Pan, C. M.; Baran, P. S., Functionalized Olefin Cross-coupling to Construct Carbon-carbon Bonds. *Nature* **2014**, *516,* 343-348; (i) Lo, J. C.; Yabe, Y.; Baran, P. S., A Practical and Catalytic Reductive Olefin Coupling. *J. Am. Chem. Soc.* **2014**, *136,* 1304-1307; (j) Dao, H. T.; Li, C.; Michaudel, Q.; Maxwell, B. D.; Baran, P. S., Hydromethylation of Unactivated Olefins. *J. Am. Chem. Soc.* **2015**, *137,* 8046-8049; (k) Gui, J.; Pan, C. M.; Jin, Y.; Qin, T.; Lo, J. C.; Lee, B. J.; Spergel, S. H.; Mertzman, M. E.; Pitts, W. J.; La Cruz, T. E.; Schmidt, M. A.; Darvatkar, N.; Natarajan, S. R.; Baran, P. S., Practical Olefin Hydroamination with Nitroarenes. *Science* **2015**, *348,* 886-891; (l) Yan, M.; Lo, J. C.; Edwards, J. T.; Baran, P. S., Radicals: Reactive Intermediates with Translational Potential. *J. Am. Chem. Soc.* **2016**, *138,* 12692-12714; (m) Lo, J. C.; Kim, D.; Pan, C. M.; Edwards, J. T.; Yabe, Y.; Gui, J.; Qin, T.; Gutierrez, S.; Giacoboni, J.; Smith, M. W.; Holland, P. L.; Baran, P. S., Fe-Catalyzed C-C Bond Construction from Olefins via Radicals. *J. Am. Chem. Soc.* **2017**, *139,* 2484-2503; (n) King, S. M.; Ma, X.; Herzon, S. B., A Method for the Selective Hydrogenation of Alkenyl Halides to Alkyl Halides. *J. Am. Chem. Soc.* **2014**, *136,* 6884-6887; (o) Ma, X.; Herzon, S. B., Non-classical Selectivities in the Reduction of Alkenes by Cobalt-mediated Hydrogen Atom Transfer. *Chem. Sci.* **2015**, *6,* 6250-6255; (p) Ma, X.; Herzon, S. B., Intermolecular Hydropyridylation of Unactivated Alkenes. *J. Am. Chem. Soc.* **2016**, *138,* 8718-8721; (q) Crossley, S. W. M.; Barabé, F.; Shenvi, R. A., Simple, Chemoselective, Catalytic Olefin Isomerization. *J. Am. Chem. Soc.* **2014**, *136,* 16788-16791; (r) Iwasaki, K.; Wan, K. K.; Oppedisano, A.; Crossley, S. W. M.; Shenvi, R. A., Simple, Chemoselective Hydrogenation with Thermodynamic Stereocontrol. *J. Am. Chem. Soc.* **2014**, *136,* 1300-1303; (s) Green, S. A.; Matos, J. L. M.; Yagi, A.; Shenvi, R. A., Branch-Selective Hydroarylation: Iodoarene–Olefin Cross-Coupling. *J. Am. Chem. Soc.* **2016**, *138,* 12779-12782; (t) Obradors, C.; Martinez, R. M.; Shenvi, R. A., Ph(*i*-PrO)SiH_2: An Exceptional Reductant for Metal-Catalyzed Hydrogen Atom Transfers. *J. Am. Chem. Soc.* **2016**, *138,* 4962-4971; (u) Matos, J. L. M.; Vasquez-Cespedes, S.; Gu, J.; Oguma, T.; Shenvi, R. A., Branch-Selective Addition of Unactivated Olefins into Imines and Aldehydes. *J. Am. Chem. Soc.* **2018**, *140,* 16976-16981; (v) Green, S. A.; Huffman, T. R.; McCourt, R. O.; van der Puyl, V.; Shenvi, R. A., Hydroalkylation of Olefins To Form Quaternary Carbons. *J. Am. Chem. Soc.* **2019**, *141,* 7709-7714; (w) Wang, Y. Y.; Bode, J. W., Olefin Amine (OLA) Reagents for the Synthesis of Bridged Bicyclic and Spirocyclic Saturated N-Heterocycles by Catalytic Hydrogen Atom Transfer (HAT) Reactions. *J. Am. Chem. Soc.* **2019**, *141,* 9739-9745; (x) Zhou, X. L.; Yang, F.; Sun, H. L.; Yin, Y. N.; Ye, W. T.; Zhu, R., Cobalt-Catalyzed Intermolecular Hydrofunctionalization of Alkenes: Evidence for a Bimetallic Pathway. *J. Am. Chem. Soc.* **2019**, *141,* 7250-7255; (y) Sun, H.-L.; Yang, F.; Ye, W.-T.; Wang, J.-J.; Zhu, R., Dual Cobalt and Photoredox Catalysis Enabled Intermolecular Oxidative Hydrofunctionalization. *ACS Catalysis* **2020**, 4983-4989; (z) Wu, B.; Zhu, R., Radical Philicity Inversion in Co- and Fe-Catalyzed Hydrogen-Atom-Transfer-Initiated Cyclizations of Unsaturated Acylsilanes. *ACS Catalysis* **2020**, *10,* 510-515.

10. (a) Shevick, S. L.; Obradors, C.; Shenvi, R. A., Mechanistic Interrogation of Co/Ni-Dual Catalyzed Hydroarylation. *J. Am. Chem. Soc.* **2018**, *140,* 12056-12068; (b) Tokuyasu, T.; Kunikawa, S.; Masuyama, A.; Nojima, M., Co(III)-alkyl complex- and Co(III)-alkylperoxo complex-catalyzed triethylsilylperoxidation of alkenes with molecular oxygen and triethylsilane. *Org. Lett.* **2002**, *4,* 3595-3598; (c) Kim, D.; Rahaman, S. M. W.; Mercado, B. Q.; Poli, R.; Holland, P. L., Roles of Iron Complexes in Catalytic Radical Alkene Cross-Coupling: A Computational and Mechanistic Study. *J. Am. Chem. Soc.* **2019**, *141,* 7473-7485; (d) Jiang, H.; Lai, W.; Chen, H., Generation of Carbon Radical from Iron-Hydride/Alkene: Exchange-Enhanced Reactivity Selects the Reactive Spin State. *ACS Catalysis* **2019**, *9,* 6080-6086.

11. (a) Shigehisa, H.; Aoki, T.; Yamaguchi, S.; Shimizu, N.; Hiroya, K., Hydroalkoxylation of Unactivated Olefins with Carbon Radicals and Carbocation Species as Key Intermediates. *J. Am. Chem. Soc.* **2013**, *135,* 10306-10309; (b) Shigehisa, H.; Koseki, N.; Shimizu, N.; Fujisawa, M.; Niitsu, M.; Hiroya, K., Catalytic Hydroamination of Unactivated Olefins Using a Co Catalyst for Complex Molecule Synthesis. *J. Am. Chem. Soc.* **2014**, *136,* 13534-13537; (c) Shigehisa, H.; Hayashi, M.; Ohkawa, H.; Suzuki, T.; Okayasu, H.; Mukai, M.; Yamazaki, A.; Kawai, R.; Kikuchi, H.; Satoh, Y.; Fukuyama, A.; Hiroya, K., Catalytic Synthesis of Saturated Oxygen Heterocycles by Hydrofunctionalization of Unactivated Olefins: Unprotected and Protected Strategies. *J. Am. Chem. Soc.* **2016**, *138,* 10597-10604; (d) Date, S.; Hamasaki, K.; Sunagawa, K.; Koyama, H.; Sebe, C.; Hiroya, K.; Shigehisa, H., Catalytic Direct Cyclization of Alkenyl Thioester. *ACS Catalysis* **2020**, *10,* 2039-2045; (e) Shigehisa, H., Functional Group Tolerant Markovnikov-Selective Hydrofunctionalization of Unactivated Olefins Using a Cobalt Complex as Catalyst. *Synlett* **2015**, *26,* 2479-2484; (f) Touney, E. E.; Foy, N. J.; Pronin, S. V., Catalytic Radical-Polar Crossover Reactions of Allylic Alcohols. *J. Am. Chem. Soc.* **2018**, *140,* 16982-16987.

12. With the exception of the following two examples, the enantioselective catalysis related to TM-HAT was reported as a preprint. see: Song, L.; Fu, N.; Ernst, B. G.; Lee, W.-H.; Frederick, M. O.; DiStasio Jr, R. A.; Lin, S., Dual Electrocatalysis Enables Enantioselective Hydrocyanation of Conjugated Alkenes. *ChemRxiv* **2019**, 10.26434/chemrxiv.9784625.v9784621.

13. Discolo, C. A.; Touney, E. E.; Pronin, S. V., Catalytic Asymmetric Radical–Polar Crossover Hydroalkoxylation. *J. Am. Chem. Soc.* **2019**, 17527-17532.

14. Shen, X.; Chen, X.; Chen, J.; Sun, Y.; Cheng, Z.; Lu, Z., Ligand-promoted cobalt-catalyzed radical hydroamination of alkenes. *Nature Communications* **2020**, *11,* 783.

15. The catalytic enantioselective hydroalkoxylation of alkenes is very rare. List reported the enantioselective organocatalytic hydroalkoxylation of disubstituted alkenyl alcohols. We and Pronin used monosubstituted alkenyl alcohols. For List's report, see: Tsuji, N.; Kennemur, J. L.; Buyck, T.; Lee, S.; Prévost, S.; Kaib, P. S. J.; Bykov, D.; Farès, C.; List, B., Activation of olefins via asymmetric Brønsted acid catalysis. *Science* **2018**, *359*, 1501-1505.

16. Niimi, T.; Uchida, T.; Irie, R.; Katsuki, T., Highly Enantioselective Cyclopropanation with Co(II)-Salen Complexes: Control ofcis- andtrans-Selectivity by Rational Ligand-Design. *Adv. Synth. Catal.* **2001**, *343,* 79-88.

17. Umemoto, T.; Harasawa, K.; Tomizawa, G.; Kawada, K.; Tomita, K., Syntheses and Properties of N-Fluoropyridinium Salts. *Bull. Chem. Soc. Jpn.* **1991**, *64,* 1081-1092.

18. (a) Trifluoroethanol also accelerates the dissolution of **3** in the reaction mixture, even at low temperature; (b) The use of carefully degassed mixed solvent was essential for high yields and enantioselectivity (see Supporting Information).

19. (a) Although Sawamura synthesized **2a** in 39% yield and 71% ee by a different method, they did not mentione the absolute configuration. We determined the absolute configuration of this compound by chemical transformation from a known compound; see Supporting information. For Sawamura's report, See: Murayama, H.; Nagao, K.; Ohmiya, H.; Sawamura, M., Copper(I)-catalyzed intramolecular hydroalkoxylation of unactivated alkenes. *Org. Lett.* **2015**, *17*, 2039-41; (b) **2a** was intact for 24 h under the reaction conditions. Thus, the enantioselective decomposition of the product can be ruled out.

20. Schaus, S. E.; Brandes, B. D.; Larrow, J. F.; Tokunaga, M.; Hansen, K. B.; Gould, A. E.; Furrow, M. E.; Jacobsen, E. N.,

Highly selective hydrolytic kinetic resolution of terminal epoxides catalyzed by chiral (salen)Co(III) complexes. Practical synthesis of enantioenriched terminal epoxides and 1,2-diols. *J. Am. Chem. Soc.* **2002**, *124,* 1307-1315.
21. Nagata, T.; Yorozu, K.; Yamada, T.; Mukaiyama, T., Enantioselective Reduction of Ketones with Sodium Borohydride, Catalyzed by Optically Active(β-Oxoaldiminato)cobalt(II) Complexes. *Angew. Chem. Int. Ed.* **1995**, *34,* 2145-2147.
22. The runs resulting in less than moderate yields tended to have a considerable amount of recovered starting material together with a small amount of byproduct; See SI in detail.
23. Use of phenylsilane could invoke the silylation of the hydroxyl group, a much weaker nucleophile, before the cylization. This would lead to the Co(IV)-C bond cleavage to form a Co(II) speices and an unstable planar secondary carbocation, followed by unselective capture by a silyl ether. see: (a) Yasuhiko, G.; Yoshihiro, Y.; Taketo, I.; Tohru, Y., Convenient and Selective Preparation of Mono-alkoxyphenylsilanes from Phenylsilane and Alcohols. Chem. Lett. 2006, 35, 714-715.; (b) Fujita, S.; Abe, M.; Shibuya, M.; Yamamoto, Y., Intramolecular Hydroalkoxylation of Unactivated Alkenes Using Silane-Iodine Catalytic System. Org. Lett. 2015, 17, 3822-3825.
24. The reversibility of the HAT step was proved by a deuterium experiment; see SI.
25. Eisenberg, D. C.; Norton, J. R., Hydrogen-Atom Transfer Reactions of Transition-Metal Hydrides. *Isr. J. Chem.* **1991**, *31,* 55-66.
26. The actual oxidant of **5** has remained unclear, though it is assumed assumed to be **3** or a cationic cobalt(III) complex. .
27. (a) Topich, J.; Halpern, J., Organobis(dioximato)cobalt(IV) Complexes: Electron Paramagnetic Resonance Spectra and Electronic Structures. *Inorg. Chem.* **1979**, *18,* 1339-1343; (b) Halpern, J.; Topich, J.; Zamaraev, K. I., Electron Paramagnetic Resonance Spectra and Electronic Structures of Organobis(dimethylglyoximato)cobalt(IV) Complexes. *Inorg. Chim. Acta* **1976**, *20,* L21-L24; (c) Vol'pin, M. E.; Levitin, I. Y.; Sigan, A. L.; Halpern, J.; Tom, G. M., Reactivity of Organocobalt(IV) Chelate Complexes Toward Nucleophiles: Diversity of Mechanisms. *Inorg. Chim. Acta* **1980**, *41,* 271-277; (d) Magnuson, R. H.; Halpern, J.; Levitin, I. Y.; Vol'pin, M. E., Stereochemistry of the Nucleophilic Cleavage of Cobalt–carbon Bonds in Organocobalt(IV) Compounds. *J. Chem. Soc., Chem. Commun.* **1978**, 44-46; (e) Abley, P.; Dockal, E. R.; Halpern, J., Oxidative Cleavage of Cobalt-carbon Bonds in Organobis(dimethylglyoximato)cobalt Compounds. *J. Am. Chem. Soc.* **1972**, *94,* 659-660; (f) Halpern, J.; Chan, M. S.; Hanson, J.; Roche, T. S.; Topich, J. A., Detection and Characterization of Radical Cations Produced by One-electron Chemical and Electrochemical Oxidations of Organocobalt Compounds. *J. Am. Chem. Soc.* **1975**, *97,* 1606-1608; (g) Anderson, S. N.; Ballard, D. H.; Chrzastowski, J. Z.; Dodd, D.; Johnson, M. D., Inversion of Configuration in the Nucleophilic Displacement of Cobalt from Alkylcobalt(IV) Complexes and Its Relevance to the Halogenation of the Corresponding Alkylcobalt(III) Complexes. *J. Chem. Soc., Chem. Commun.* **1972**, 685-686.
28. Lande, S. S.; Kochi, J. K., Formation and Oxidation of Alkyl Radicals by Cobalt(III) Complexes. *J. Am. Chem. Soc.* **1968**, *90,* 5196-5207.
29. Samsel, E. G.; Kochi, J. K., Radical Chain Mechanisms for Alkyl Rearrangement in Organocobalt Complexes. *J. Am. Chem. Soc.* **1986**, *108,* 4790-4804.
30. Li, S.; de Bruin, B.; Peng, C. H.; Fryd, M.; Wayland, B. B., Exchange of organic radicals with organo-cobalt complexes formed in the living radical polymerization of vinyl acetate. *J. Am. Chem. Soc.* **2008**, *130,* 13373-13381.
31. Mayr, H.; Ofial, A. R., The Reactivity–Selectivity Principle: An Imperishable Myth in Organic Chemistry. *Angew. Chem. Int. Ed.* **2006**, *45,* 1844-1854.
32. Buschmann, H.; Scharf, H.-D.; Hoffmann, N.; Esser, P., The Isoinversion Principle—a General Model of Chemical Selectivity. *Angew. Chem. Int. Ed.* **1991**, *30,* 477-515.
33. Andrade, E. N. D. C., The Viscosity of Liquids. *Nature* **1930**, *125,* 309-310.
34. de Bruin, B.; Dzik, W. I.; Li, S.; Wayland, B. B., Hydrogen-Atom Transfer in Reactions of Organic Radicals with [CoII(por)]. (por=Porphyrinato) and in Subsequent Addition of [Co(H)(por)] to Olefins. *Chem. Eur. J.* **2009**, *15,* 4312-4320.
35. Wheeler, S. E.; Seguin, T. J.; Guan, Y.; Doney, A. C., Noncovalent Interactions in Organocatalysis and the Prospect of Computational Catalyst Design. *Acc. Chem. Res.* **2016**, *49,* 1061-1069.